Applied Catalysis A, General 547 (2017) 105–114

Contents lists available at ScienceDirect

Applied Catalysis A, General

journal homepage: www.elsevier.com/locate/apcata

Feature Article

Nanoscale Ziegler catalysts based on bis(acetylacetonate)nickel in the arene hydrogenation reactions

Yuliya Yu. Titova*, Fedor K. Schmidt

Department of Chemistry, Irkutsk State University, 1 K. Marx str., 664003 Irkutsk, Russia

ARTICLE INFO

Keywords:
Hydrogenation
Arene
Nickel catalysts
Nanoparticle
Adsorption constant

ABSTRACT

The turnover frequencies of catalytic systems based on $Ni(acac)_2$–$AlEt_3$ or $AlEt_2(OEt)$ in the hydrogenation of benzene and its methyl-substituted homologs (toluene, three isomers of xylene, and 1,3,5-trimethylbenzene) have been determined at temperatures of 80–120 °C, initial P_{H2} = 15 bar, and different ratios of Al/Ni. The size and nature of the nanoparticles forming in the systems based on $Ni(acac)_2$–$AlEt_3$ or $AlEt_2(OEt)$ under the benzene hydrogenation condition shave been resolved by high-resolution electron microscopy and X-ray microanalysis. This study included the performance of competitive hydrogenation reactions of benzene with toluene or three xylene isomers. The relative adsorption constants of toluene and three xylene isomers have been determined and the stereochemistry of the hydrogen addition to the arene ring has also been elucidated.

1. Introduction

One of the main goals of both fundamental and applied catalysis is the development of highly active, selective, and productive catalysts for industrially significant processes. To this end, a deep understanding of the elemental composition, size, and electronic structure of the active centers as well as the ligand shell and other factors that affect the quantitative characteristics (turnover frequency (TOF) and turnover number (TON)) of the catalytic systems is needed. In this sense, nanoscale materials possess a unique potential since they offer the opportunity to analyse and control all the above factors almost at the molecular level [1]. In particular, the Ziegler hydrogenation systems, the nanoscale nature of which was proved in modern studies [2–11], allow modification of the catalyst composition and accordingly of the quantitative characteristics over a wide range [12,13].

In 2010 the research group of Prof. R.G. Finke presented a comprehensive review of the literature dedicated to Ziegler hydrogenation catalysts [14], in which the merits and demerits of these systems, the possibilities of physical and chemical research methods in this field, and current trends in the study of such catalysts were discussed in details. In this article, in particular, the several problems were listed for which a special attention in further studies of such systems should be given. Namely: (1) how any changes in the initial variables of the catalytic system formation influence its composition, structure and catalytic activity; (2) what is the true nature of the formed catalytically active system (homogeneous or heterogeneous), as well as details of the catalytic hydrogenation mechanism; (3) how many atoms of a transition metal (and not only a transition metal) are included in the composition of catalytic active centers and what is their degree of oxidation; (4) the role of a cocatalyst in each particular case and other components of the system, including uncontrolled ones. In addition, the authors recommended collecting of the additional kinetic data for many Ziegler hydrogenation systems with taking into account the methodology of active catalyst formation. In conclusion, it was noted that «Additional catalytic application, fundamental kinetic, spectroscopic, as well as other studies are strongly encouraged, regardless of whether Ziegler nanoclusters are the true catalysts in all, or even selected, cases» [14].

Significant progress in the understanding of the structure of nanoscale Ziegler hydrogenation catalysts has been achieved in the last decades [2–11,15,16]. In particular, the role of organoaluminium compounds and the products of their transformations—formed by the reaction of an initial transition metal complex with the organoaluminium compound—in the generation of a ligand shell stabilizing the transition metal nanoparticles was substantiated [4–7,11,16]. The necessity to introduce a proton donor (H_2O, ROH, acetyl acetone, etc.) in the catalytic system to enhance the hydrogenation catalyst activity was also shown [10,11,15,16]. These studies were carried out using styrene, 1-hexene and cyclohexene hydrogenation as the model reaction. Nevertheless, the issue of the composition and structure of a true catalytically active center has not been fully resolved yet.

In addition, despite the research of the Ziegler hydrogenation catalysts were being carried out for more than half a century, there are a little of information about arenes hydrogenation on such systems. Analysis of the literature allowed to find only a few works devoted to

* Corresponding author.
E-mail address: ytitova60@gmail.com (Y.Y. Titova).

http://dx.doi.org/10.1016/j.apcata.2017.08.029
Received 30 June 2017; Received in revised form 11 August 2017; Accepted 21 August 2017
Available online 25 August 2017
0926-860X/ © 2017 Published by Elsevier B.V.

this issue, for example [17–22]. In addition, there are review articles [23,24], where examples of the investigation of Ziegler systems are discussed among other things. Nevertheless, the fundamental research of the nature of catalytically active forms in the catalysis of arenes hydrogenation are virtually absent, with the exception of [18,21,22]. The authors of these papers presented convincing evidences of the nanosized nature of catalytically active centers. Quantitative data, namely, values of TTO (100,000 total turnover) are presented in several articles only.

Nevertheless, exactly the catalysts of the Ziegler type have found widespread use in industrial processes such as the hydrogenation of butadiene-styrene copolymers [25]. Thus, it can be assumed that the Ziegler catalysts for arene hydrogenation could be used, for example, in fine organic synthesis, where one of the steps is a benzene ring hydrogenation.

Moreover, the process of hydrogenation of benzene and its homologs is important both from an industrial and environmental point of view. It is sufficient to mention the benzene hydrogenation to cyclohexane and cyclohexene and the phenol hydrogenation to cyclohexanol [26], or the issues related to the diesel fuel production with a low content of aromatic hydrocarbons. The results published in the literature mainly concern the effect of the catalytic system composition on the yield of the hydrogenation products [14,27–30]. However, quantitative data about the TOF and TON values in the arene hydrogenation reaction are virtually absent.

The aim of this study was to determine the catalytic properties of Ziegler systems based on $Ni(acac)_2$ from a quantitative standpoint in the hydrogenation of benzene and its methyl homologs, including the hydrogenation under competitive conditions, and to establish the nature of the particles that are responsible for the catalytic process. The application of the competitive hydrogenation method to the Ziegler hydrogenation catalysts have a special importance, both from the fundamental point of view, since it allowed to compare the reactivity of arenes under strongly identical conditions, and with the applied point of view, for those cases when the arene substrates contains of the aromatic impurities.

2. Experimental

2.1. General procedures

Benzene, toluene, xylenes (*o-,m-, p-*), *n*-hexane were purified by the standard protocols applied for handling with organometallic compounds [31]. To reach a deeper drying, benzene and toluene were additionally distilled under $LiAlH_4$ (xylenes under CaH_2) on the rectifying column and stored under argon in sealed ampoules over molecular sieves 4 A. Concentration of water in the solvents, measured by Fischer method [32], was about 1 mmol/l.

Argon was purified from moisture and oxygen by consecutive passing through the columns filled with P_2O_5, granulated alkali, molecular sieves SAA and powder copper heated to 200 °C.

Hydrogen (Brand 1, National standard No. P51673-2000) was purified from oxygen and water traces by consecutive passing through the columns filled with nickel-chromium catalyst and SAA zeolites.

Triethylaluminum [33] was purified by distillation in vacuum at 48 − 49°C/1 Hg mm. It was stored in ampoules under argon atmosphere. $AlEt_3$ was diluted in Schlenk tube in hexane or in octane under argon. Concentration of $AlEt_3$ solution was determined by volumetric analysis removing aliquot of the solution with water. Purity of $AlEt_3$ was checked by the PMR method: δ_{CH_2} = 0.45 ppm (q, ^1J = 8.24 Hz), δ_{CH_3} = 1.22 ppm (t, ^1J = 8.24 Hz).

Diethyl aluminum ethoxide ($AlEt_2(OEt)$) was obtained from $AlEt_3$ solution in hexane by dropping of the desired quantity of C_2H_5OH under continuous cooling at T = −10 °C and stirred in an argon atmosphere.

Ethanol was refluxed over freshly calcinated CaO under argon and distilled over needle column. Further, it was boiled and distilled over sodium collecting the fraction, which boiled at 78 °C [34].

The samples of nickel bis(acetylacetonate) ($Ni(acac)_2$) were synthesized according to the protocols described in [11,35]. The purity of the $Ni(acac)_2$ was determined by thermogravimetric analysis combined with differential scanning calorimetry on a STA 449 F3 Jupiter derivatograph (Netzch, Germany) under the following conditions: rate of nitrogen feeding was 30 ml/min, rate of heating was 5 K/min.

2.2. Experimental protocols

2.2.1. Catalyst formation

The sample of $Ni(acac)_2$ (4×10^{-4}mol, 0.1028 g), benzene or other arene (36 ml) were sequentially placed into preliminarily vacuumed in the thermostatically controlled flask filled with hydrogen. The reaction mixture was stirred for 25 min until a transparent light-green solution was formed. To the solution obtained, $AlEt_3$ (or $AlEt_2(OEt)$) solution in *n*-hexane (4 ml) were added, the varied ratios of Al/Ni being 1–10 (general volume of system is 40 ml). The reaction of catalyst formation was monitored by gas evolution and UV-spectroscopy (method of sequential approximation).

2.2.2. Hydrogenation experiments

The experiments on hydrogenation were carried out in an autoclave (Reactor System M-FGA-ST-MDF-AC-R, “REXO Engineering”, S. Korea) provide with mechanical stirrer, manometer, two gas lines, sampling device and controller (Control System CS-1000, “REXO Engineering”, S. Korea), at specified temperature (80–120 °C), initial hydrogen pressure (15 bar) and vigorous stirring (500–750 turn/min) which provides the process flow in the kinetic region.

The generated in situ reaction mixture with hydrogenated arenes (view “Catalyst formation”) was placed into an autoclave preliminarily filled with hydrogen. The hydrogenation reaction was monitored by pressure drop on a monometer and the samples were analyzed by GLC technique. The analysis was performed on a «Khromatek-Kristall 5000.2” instrument (“Khromatek”, Russia) equipped with flame-ionization detector using HP Carbowax 20 M capillary column (30 m length, 0.53 mm diameter), and GCMS-QP-2010 mass spectrometer (Shimadzu, Japan).

TOF was estimated as the number of molecules reacted at nickel mole per time (in min). Relative error of the TOF value that determined from three to five parallel experiments is not more than 5%.

The TON values for the considered catalytic systems were not given in the first variant of the article. This is due to the fact that the technical capabilities of our autoclave allow us to carry out the hydrogenation process within 3 ± 0.5 h. So we were not able to determine the maximum lifetime of the catalyst (even with acceptably low catalyst concentrations we were not able to achieve the complete deactivation of the catalytic activity during the indicated time period). Accordingly, to this, we refrained from comparing our TON values with previously published parameters for heterogeneous catalytic systems.

2.3. Research methods

2.3.1. ESR-spectroscopy

The ESR spectra were recorded on an ESP 70-03 XD/2 spectrometer (KBST Enterprise, Republic of Belarus) at working frequency of 9.3 GHz; DFPH was used as reference.

2.3.2. UV-spectroscopy

The UV spectra were recorded on a SF 2000 (Russia) spectrometer in the range 280–430 nm in a seamless cuvette (0.01 cm).

2.3.3. Transmission electron microscopy

Samples were collected from the $Ni(acac)_2$–$5AlEt_3$ (or $Ni(acac)_2$–$4AlEt_2(OEt)$) reaction system both before and during benzene

hydrogenation. The solutions obtained were diluted with benzene to one-thirty of their original concentration. A drop of the diluted solution was applied to a carbonized copper grid (200 mesh) and dried in a glovebox at ambient temperature under an inert atmosphere.

High-resolution transmission electronic microscopy (HRTEM, Tecnai G2, FEI, USA) images were obtained using an accelerating voltage of 200 kV, and recorded using a CCD camera (Soft Imaging System, Germany). The samples were then subjected to chemical microanalysis and annular dark-field imaging. Local elemental analysis was performed using energy dispersive X-ray spectroscopy (EDX, Phoenix) using a Si (Li) detector with an energy resolution of approximately 130 eV. The parameters of the particle images were measured using the iTEM 5.0 and DigitalMicrographs 1.94.1613 software. Periodic structures and image filtration were analyzed using Fourier methods, i.e., fast Fourier transformation (FFT) and inverse fast Fourier transformation (IFFT). The inter- layer distances were determined using the image intensity profiles obtained using the DigitalMicrographs 1.94.1613 software. Diffraction patterns was processing using RDFTools plugin for DigitalMicrographs 1.94.1613 software. The average particle diameters were determined by measuring 250–350 particles on enlarged micrographs, and calculated using the following formula:

$$\bar{d} = \frac{\sum d_i}{n}$$

3. Results

3.1. Influence of the catalytic system composition on the catalytic properties

The dark brown solution formed by reacting triethylaluminium with bis(acetylacetonate)nickel was found to be active in the hydrogenation reaction of benzene at temperatures higher than 40 °C. In particular, the hydrogenation rates suitable for the autoclave procedure were observed in the temperature range 80–150 °C. The use of $AlEt_3$ as reducing agent for the $Ni(acac)_2$ systems led to an increase of the TOF by approximately two orders of magnitude compared to the nickel black formed upon reduction of $Ni(acac)_2$ by hydrogen. For example, the benzene hydrogenation after the $Ni(acac)_2$ reduction promoted by hydrogen was characterized by a TOF = 0.03 min^{-1} at T = 120 °C and P_{H2} = 15 bar, whereas a TOF of ~3 min^{-1} was obtained with the catalytic system based on $Ni(acac)_2$–$AlEt_3$ (Al/Ni = 4) under the same conditions. It should also be noted that the activity of the investigated system at the optimum Al/Ni ratio was more than one order of magnitude higher than that of the heterogeneous nickel catalysts such as Ni/γ-Al_2O_3 [36,37].

In our opinion, the most exact value of TOF should be defined as the ratio (mol arene)/(number of active centers-mines). However, since the number of active centers was not determined yet at this stage of the study, the traditional method of determining TOF was applied. Although, of course, since the systems under investigation can be considered as heterogeneous, the TOF values can be calculated as (mol arene)/(surface area of the all particles-mines). A similar calculation for the most active systems is presented in SI(A1) for comparison.

The TOF value of the benzene hydrogenation was primarily determined by the value of the molar ratio of $AlEt_3$/$Ni(acac)_2$ as in the alkene hydrogenation. This relationship was characterized by a sharp peak when Al/Ni = 4 (Fig. 1).

The data presented for the $Ni(acac)_2$-$AlEt_2(OEt)$ system at Fig. 1 were obtained at T = 120 °C, and for $Ni(acac)_2$-$AlEt_3$ system at a T = 100 °C. The TOF values for the $Ni(acac)_2$-$AlEt_3$ system obtained at T = 120 °C was 1.5–1.7 times higher than the data obtained at 100 °C; the kinetic curve also passed through the maximum observed at the ratio Al/Ni = 4.

A different dependence of the TOF on the Al/Ni ratio was observed when $AlEt_3$ was replaced by $AlEt_2(OEt)$ (Fig. 1). It can be seen that for systems based on $Ni(acac)_2$–$AlEt_2(OEt)$ an increase in activity was

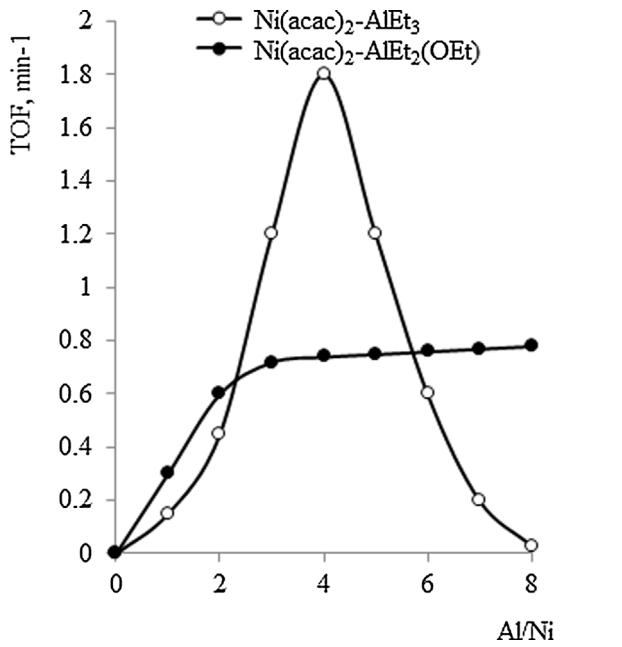

Fig. 1. The dependences of TOF of nickel catalysts on the basis of $Ni(acac)_2$ − $AlEt_3$ and $Ni(acac)_2$ − $AlEt_2(OEt)$ upon Al/Ni ratio: [Ni] = $1{\cdot}10^{-2}$ mol/l, [benzene] = 10.1 mol/l, P_{H2} = 15 bar, T = 100 °C for $Ni(acac)_2$ − $AlEt_3$ and T = 120 °C for $Ni(acac)_2$ − $AlEt_2(OEt)$.

observed at values of Al/Ni ≤ 4, while for Al/Ni = 4–10 the activity remained practically constant. These results are of great importance in the study of the kinetics of the process because when 4 ≤ Al/Ni ≤ 10, the concentration of the organoaluminium material has virtually no effect on the activity of the catalyst system at the stage of the catalyst formation.

The benzene hydrogenation rate was directly proportional to the Ni $(acac)_2$ concentration and hydrogen pressure, while it did not depend on the concentration of benzene at $C_{C6H6} > 1 \times 10^{-2}$ mol/L (Fig. S1.1-1.4 in Supplementary Material (S)).

The values of both effective activation energy (E_a, kcal/mol) and pre-exponential factor (A, min^{-1}) for the systems based on Ni $(acac)_2$–$AlEt_3$ ($AlEt_2(OEt)$) are given in Table 1 (Fig. S1.5 for the Ni $(acac)_2$–5$AlEt_2(OEt)$ system in the benzene hydrogenation).

The analysis of the data in Table 1 suggests that the effective activation energy as well as the pre-exponential factor increase with the increasing degree of substitution of the benzene ring in the order benzene < toluene < *p*-xylene for the systems based on Ni(aca-c)$_2$–$AlEt_2(OEt)$.

The quantitative characteristic of the catalytic systems based on Ni $(acac)_2$–$AlEt_3$ and $Ni(acac)_2$–$AlEt_2(OEt)$ in the hydrogenation of individual arenes as well as the competitive hydrogenation of benzene and/with alkyl benzenes (toluene and xylenes) are given in Table 2.

Table 2 (column 2) shows that the TOF of the hydrogenation of aromatic molecules decreases in the order benzene > toluene > *p*-xylene > *m*-xylene ≥ *o*-xylene > mesitylene in the investigated

Table 1
Parameters of Arrhenius equation in the hydrogenation of benzene and its homologues.

Arene	A, min^{-1}	E_a, kkal/mol	A, min^{-1}	E_a, kkal/mol
	$Ni(acac)_2$–4$AlEt_3$		$Ni(acac)_2$–5$AlEt_2(OEt)$	
Benzene	$1.70{\cdot}10^6$	10.30 ± 0.4	$8.70{\cdot}10^5$	10.50 ± 0.4
Toluene			$1.15{\cdot}10^7$	13.00 ± 0.5
p-Xylene			$1.55{\cdot}10^8$	15.50 ± 0.6

Reaction conditions: [Ni] = $1{\cdot}10^{-2}$ mol/l, [arene] = 10.1 mol/l, P_{H2} = 15 bar, T = 80 − 120 °C.

Table 2
Quantitative characteristics of the $Ni(acac)_2$–$AlEt_3$ and $Ni(acac)_2$–$AlEt_2(OEt)$ catalytic systems in individual arenes hydrogenation and competitive hydrogenation of benzene and/with alkylbenzenes.

Arene	TOF, min^{-1}	$(TOF_{C6H6})/(TOF_{arene})$	TOF_{C6H6} [1,2]	TOF_{arene} [1,2]	$(TOF_{C6H6})/(TOF_{arene})$ [1]	$(K_{C6H6})/(K_{arene})$
1	2	3	4	5	6	7
$Ni(acac)_2$–4 $AlEt_3$						
Benzene	3.10	1	–	–	–	–
Toluene	1.10	2.9	2.0	0.6	3.3	1.5
o-Xylene	0.56	5.5	2.1	0.26	8.1	2.3
m-Xylene	0.60	5.2	2.2	0.28	7.8	2.6
p-Xylene	0.65	4.7	2.4	0.29	8.3	3.5
Mesitylene	0.12	25	–	–	–	–
$Ni(acac)_2$–5$AlEt_2(OEt)$						
Benzene	1.25	1.0	–	–	–	–
Toluene	0.47	2.7	0.66	0.22	3.0	1.45
o-Xylene	0.30	4.2	0.68	0.12	5.7	2.10
m-Xylene	0.33	3.8	0.71	0.12	5.9	2.20
p-Xylene	0.36	3.5	0.79	0.13	6.1	3.90

Reaction conditions: [Ni] = $1{\cdot}10^{-2}$ mol/l, V = 40 ml, P_{H2} = 15 bar, T = 120 °C.
[1] competitive hydrogenation.
[2] (mol % C_6H_6)/(mol % arene) = 1.

temperature range. A decrease in the TOF values caused by the presence of additional methyl groups was not surprising. This fact was previously mentioned for heterogeneous catalysts, for example supported platinum [38], palladium [39], rhodium, cobalt [40], and nickel [41,42] systems. The main products of the benzene and toluene hydrogenation are cyclohexane and methylcyclohexane, respectively. However, trace amounts of cyclohexene and methylcyclohexene (< 0.005%) were detected by GLC technique at the initial stage of the catalytic process.

The hydrogenation of *o-, m-,* and *p*-xylenes by the described nickel Ziegler catalysts in the 50–150 °C temperature and 5–25 bar pressure ranges resulted in the formation of *cis-* and *trans*-isomers of 1,2-, 1,3-, and 1,4-dimethylcyclohexane, respectively. The isomerization and hydrogenolysis of xylenes and dimethylcyclohexanes were not observed under the employed conditions.

The aspects related to the component interaction of the studied catalytic systems have been examined by many authors by using both physical and chemical methods [10,15,43–46]. It has been shown that the organoaluminium compounds act as reductants of Ni(II) to Ni(0) species, stabilizers of nickel nanoparticles, and inhibitors of the hydrogenation activity. A nickel nanoparticle model named the Schmidt-Bönnemann model has been previously identified [4,6,10,15,43,47–49]. This model consents to explain the activating role of the proton-donating compounds in the formation of the hydrogenation catalysts. Herein, we report only the results obtained by TEM and ESR spectroscopy under the benzene hydrogenation condition for the $Ni(acac)_2$–$AlEt_3$ and $Ni(acac)_2$–$AlEt_2(OEt)$ systems investigated. The detailed data of the volumetric analysis are given in Supplementary Material (Appendix B).

3.2. Transmission electron microscopy studies

3.2.1. $Ni(acac)_2$ system after 1 h of benzene hydrogenation at T = 120 °C and P_{H2} = 15 bar

The TEM image, selected area electron diffraction (SAED) pattern, and EDX spectrum of the catalyst prepared by reduction of $Ni(acac)_2$ under hydrogen and used in the benzene hydrogenation at T = 120 °C and P_{H2} = 15 bar are given in Fig. 2.

Both crystalline particles (Fig. 2*a*) and amorphous formations were recorded on the microphotographs. The particle sizes, the pattern derived from the electron diffraction investigation of the different fields of the sample, as well as the results of the local elemental analysis of different parts of the $Ni(acac)_2$ sample are given in Table 3 (N1). The presence of NiO results from the partial oxidation of the sample by air oxygen during its installation into the microscope.

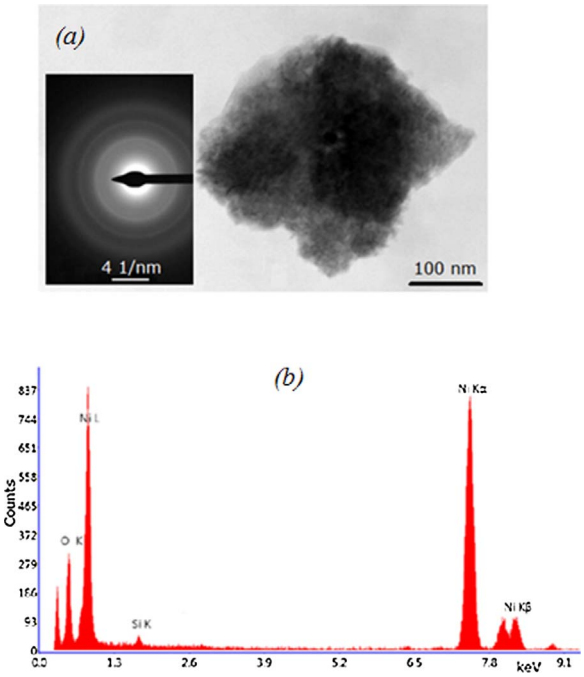

Fig. 2. TEM *(a)* particle formed by reduction of $Ni(acac)_2$ in the hydrogen, and the EDX spectrum *(b)*. The inset in *(a)* is the selected area electron diffraction (SAED) pattern.

The received TEM data together with the results of the kinetic studies indicated the presence of microscopic nickel particles, which explains the low activity observed in the benzene hydrogenation. It should be noted that the data of the UV studies demonstrated that only 50% of $Ni(acac)_2$ was reduced under the benzene hydrogenation conditions (T = 120 °C and P_{H2} = 15 bar).

Recently, it has been shown [11,15] that the particle formation was not registered by TEM after the interaction between $Ni(acac)_2$ and $AlEt_3$ at room temperature in a benzene solution (Fig. S3.1).

3.2.2. $Ni(acac)_2$–4$AlEt_3$ system after benzene hydrogenation at T = 120 °C and P_{H2} = 15 bar

The TEM image, SAED pattern, particle size distribution histogram, and EDX spectrum of the $Ni(acac)_2$–4$AlEt_3$ system after 40 min of benzene hydrogenation at T = 120 °C and P_{H2} = 15 bar are shown in Fig. 3.

Table 3
Parameters of the particles formed in $Ni(acac)_2$–*4*$AlEt_3$and $Ni(acac)_2$–*5*$AlEt_2(OEt)$ catalytic systems during benzene hydrogenation.

N	Hydrogenation time, min	$d_{min} - d_{max}$, nm	a_{verage}, nm	Ni, d/n, Å (*hkl*)	NiO, d/n, Å (*hkl*)	Elemental microanalysis, at.%	ESR spectrum parameter
1	2	3	4	6	7	9	10
$Ni(acac)_2$ (H_2)							
1	40	390–890	–	2.0382 (111)[1] 1.744 (200)[1] 1.2812 (220)[1] 1.0789 (311)[1]	2.412 (101)[2] 2.1126 (012)[2] 1.481 (110)[2] 1.477 (104)[2]	Ni – 71.01; O – 24.13; C – 4.87	–
$Ni(acac)_2$ – $4AlEt_3$							
2	40	0.6–2.5	1.38 ± 0.33		–	Ni – 4.17; Al – 4.07; O – 13.2; C – 78.56	g = 2.2[4]
3	80	1.4–3.2	2.12 ± 0.10	2.0375 (111)[1,3] 1.772 (200)[1] 1.2532 (220)[1] 1.0685 (311)[1]	–	–	g = 2.2[4]
$Ni(acac)_2$ – $5AlEt_2(OEt)$							
4	0[5]	1.5–6.0	3.77 ± 0.87	2.0462 (111)[1,3] 1.782 (200)[1] 1.2602 (220)[1,3] 1.0725 (311)[1]	–	Ni – 6.61; Al – 2.89; O – 12.82; C – 77.67	g = 2.2[4]
5	40	2.0–6.1	4.22 ± 0.54	2.0366 (111)[1] 1.759 (200)[1] 1.247 (220)[1] 1.0634 (311)[1]	–	Ni – 16.75; Al – 6.24; O – 10.25; C – 67.19	g = 2.2[4]
6	80	1.9–13.0	5.50 ± 1.81	–	–	–	g = 2.2[4]

Reaction conditions: [Ni] = $1 \cdot 10^{-2}$ mol/l, [arene] = 10.1 mol/l, V = 40 ml, P_{H2} = 15 bar, T = 120 °C.
[1] 2.034 Å (111); 1.762 Å (200), 1.246 Å (220), 1.0624 Å (311) (Ni # 00-004-0850).
[2] 2.41197 Å (101); 2.08849 Å (012), 1.47733 Å (110), 1.47607 Å (104) (NiO # 00-044-1159).
[3] 2.0413 Å (110); 1.4437 Å (200), 1.2913 Å (210) (NiAl # 00-044-1188).
[4] The intensity of the signal grew during the further hydrogenation of arene.
[5] The probe was sampled on step of the interaction of the initial components before the 15 bar of hydrogen was applied to the system.

The size of the particles in this system varied from 0.6 to 2.5 nm (Fig. 3*b*, Table 3, N2). The average particle size was 1.38 ± 0.33 nm and particles with a diameter in the range 1.4–1.2 nm were predominant.

The results of the investigation of the electron diffraction pattern of the different fields of the $Ni(acac)_2$–$4AlEt_3$ system, as well as those of the local elemental analysis of different parts of the sample are given in Table 3 (N2). According to the HRTEM and electron diffraction data, the inter-lattice distances are 2.032 and 2.04 Å (Fig. S3.2), corresponding to the (111) plane of Ni (2.034 Å, # 00-004-0850) and (110) plane of NiAl (2.0413 Å # 00-044-1188), respectively.

The sample taken after 80 min of hydrogenation was characterized by an average particle size of 2.12 ± 0.10 (Fig. S3.3, Table 3, N3). The predominant particle size was 2.0–2.1 nm. The aspherical shape of the particles, as well as the dependence of the particle size distribution (the virtually logarithmic normal distribution), indicates that the growth of the nickel particles during the hydrogenation process is due to cluster aggregation [50].

Furthermore, a weak ferromagnetic resonance signal was recorded in the ESR spectrum for this system. The intensity of this signal hardly changed during the benzene hydrogenation (Table 3, N3). Therefore, owing to $Ni(acac)_2$ and $AlEt_3$ an almost uniform system was transformed into nanoscale clusters of AlNi and Ni, which were catalytically active under benzene hydrogenation conditions (T = 120 °C and P_{H2} = 15 bar).

If it is imagined that the particles that formed in the $Ni(acac)_2$-$AlEt_3$ system consists of only nickel then the number of atoms in a metal nanoparticle at its densest packing are presented in SI(A2).

3.2.3. $Ni(acac)_2$–$5AlEt_2(OEt)$ system under room temperature and P_{H2} = 1 bar

The TEM image, SAED pattern, particle size distribution histogram, and EDX spectrum of the $Ni(acac)_2$–$5AlEt_2(OEt)$ system formed at room temperature and P_{H2} = 1 bar are shown in Fig. 4.

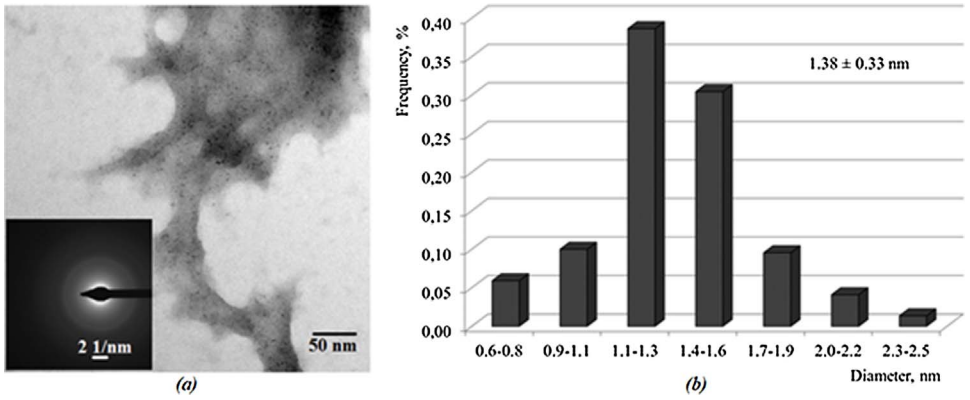

Fig. 3. TEM *(a)* particle formed in the Ni $(acac)_2$-$4AlEt_3$after benzene hydrogenation at T = 120 °C and P_{H2} = 15 bar, and *(b)* the particle-size distribution histogram. The inset in *(a)* is the selected area electron diffraction (SAED) pattern.

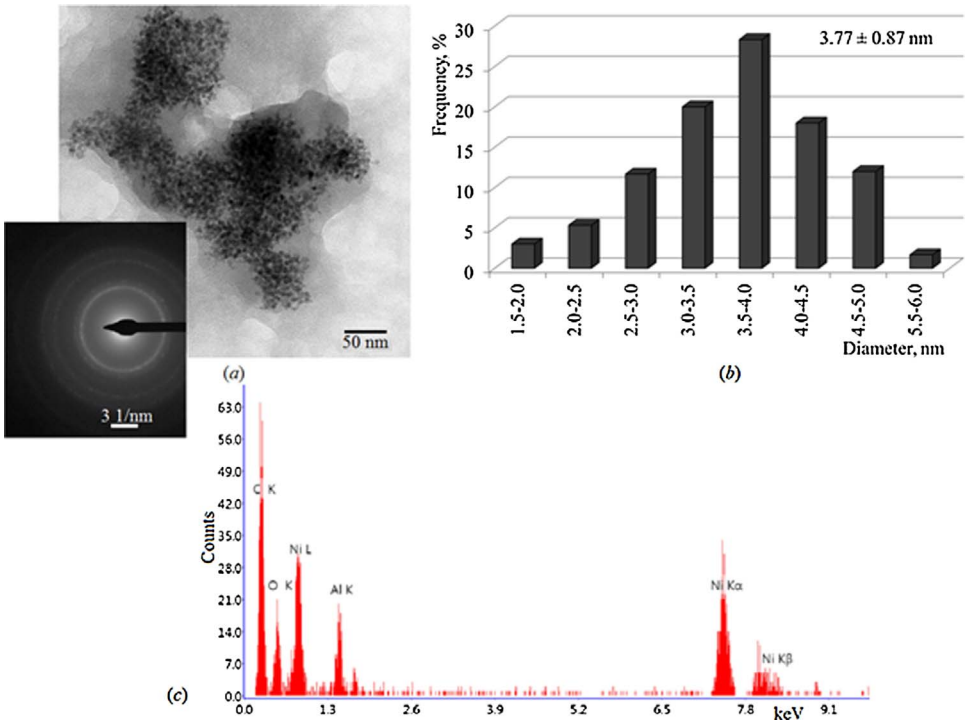

Fig. 4. TEM *(a)* particle formed in the Ni $(acac)_2$–$5AlEt_2(OEt)$ under a room temperature and P_{H2} = 1 bar, *(b)* the particle-size distribution histogram and *(c)* the EDX spectrum. The inset in *(a)* is the selected area electron diffraction (SAED) pattern.

The size of the particles varied from 1.5 to 6.0 nm (Fig. 4*b*, Table 3, N4). The average particle size formed in Ni$(acac)_2$–$5AlEt_2(OEt)$ under a hydrogen atmosphere was 3.77 ± 0.87 nm, and particles with a diameter in the range 3.0–4.5 nm were predominant. Assuming that the particles are nickel clusters, it is possible to calculate the number of atoms in a metal nanoparticle at its densest packing using an appropriate formula (equation S3.1) [4]. Here, the average diameter of the nanoparticles was 3.77 nm, which corresponded to a nickel nanoparticle containing ~2700 atoms ($Ni_{\sim 2700}$). The minimum particle size (1.5 nm) corresponded to the nucleus of a nickel nanoparticle containing 175 atoms ($Ni_{\sim 175}$). The maximum size of the particles (6.0 nm) corresponded to a nickel nanoparticle containing 11250 atoms ($Ni_{\sim 11250}$).

The pattern resulting from the electron diffraction investigation of the different fields of the Ni$(acac)_2$–$5AlEt_2(OEt)$ system, as well as the results of the local elemental analysis of different parts of the sample are given in Table 3 (N4).

A wide ferromagnetic resonance signal with low intensity was visible in the ESR spectrum of this system (Table 3).

3.2.4. Ni$(acac)_2$–$5AlEt_2(OEt)$ system after benzene hydrogenation at T = 120 °C and P_{H2} = 15 bar

The TEM image, SAED pattern, particle size distribution histogram, and EDX spectrum of the Ni$(acac)_2$–$5AlEt_2(OEt)$ system after 40 min of benzene hydrogenation at T = 120 °C and P_{H2} = 15 bar are shown in Fig. 5.

The size of the particles varied from 2.0 to 6.1 nm (Fig. 5*b*, Table 3, N5). The average particle size formed in the Ni$(acac)_2$–$5AlEt_2(OEt)$ system after 40 min of benzene hydrogenation was 4.22 ± 0.54 nm. It corresponded to nickel nanoparticles containing approximately ~3900 nickel atoms. The predominant particle size was 2.9–4.8 nm.

The pattern resulting from the electron diffraction investigation of the different fields of the Ni$(acac)_2$–$5AlEt_2(OEt)$ system, as well as the results of the local elemental analysis of different parts of the sample are given in Table 3 (N5). According to the HRTEM and electron diffraction data, the inter-lattice distance of 2.036 Å (Fig. S3.4) corresponded to the (111) plane of Ni (2.034 Å, # 00-004-0850).

The average size of the metal nanoparticles formed in the Ni $(acac)_2$–$5AlEt_2(OEt)$ system increased during the hydrogenation at T = 120 °C and P_{H2} = 15 bar, reaching the value of 5.50 ± 1.81 nm after 80 min of benzene hydrogenation. This value corresponded to nickel nanoparticles containing ~8650 nickel atoms (Fig. S3.5, Table 3, N6). The increase of the particle size in the Ni$(acac)_2$–$5AlEt_2(OEt)$ system could be due to diffuse aggregation [4]. A wide ferromagnetic resonance signal with high intensity was observed in the ESR spectrum of this system (Table 3, N6). The intensity of the ESR signal grew during the hydrogenation of benzene.

By comparing the characteristics of the nickel nanoparticles in the Ni$(acac)_2$–$4AlEt_3$ and Ni$(acac)_2$–$5AlEt_2(OEt)$ systems, a higher capacity of $AlEt_3$ to stabilize the nanoparticles compared to $AlEt_2(OEt)$ could be noted. This observation is in good agreement with the Schmidt-Bönnemann model [4,6,10,15,43,47–49].

The algorithm consisting of four techniques, which makes it possible to distinguish homogeneous catalytically active centers from nanoscale heterogeneous ones, was given in [4,51]. Namely, they are (1) kinetic experiments; (2) studies conducted by TEM; (3) experiments with poisoning of the catalyst, for example by Hg(0); (4) additional studies of the catalytic hydrogenation mechanism, taking into account the data obtained in paragraphs (1) − (3).

The analysis of the results of kinetic experiments presented above indicated that the hydrogenation rate of benzene in the presence of the catalytic systems Ni$(acac)_2$-$AlEt_3$ (or $AlEt_2(OEt)$) depends not only on the Al/Ni ratio (Fig. 1) but also on the concentration of the original Ni (II) complex (see Fig. S1.1). The observed increase in the reaction rate with an increase of the concentration of Ni$(acac)_2$ resulted from a growth in the fraction of active surface centers. The growth of catalytic activity with an increase of the concentration of $AlEt_3$ resulted from the formation of a more highly dispersed nickel catalyst. The drop in catalytic activity was the consequence of the poisoning effect of $AlEt_3$ excess.

The data obtained by the TEM and described in [11,16,35,43] and in the present article indicates that nanoscale nickel-containing particles are formed exactly during the hydrogenation of benzene directly in the autoclave. The question about the catalytic activity of the 1–4 nm particles in the hydrogenation of arenes remains opened. It is possible that the TOF values described above resulted from the presence in the

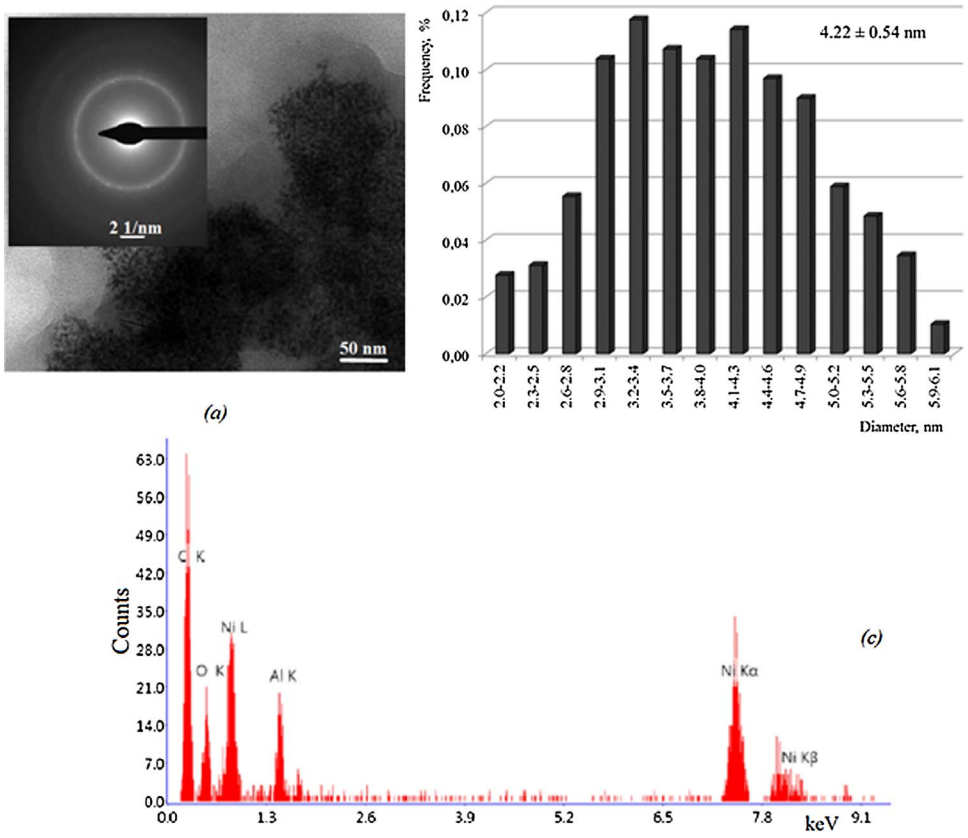

Fig. 5. TEM *(a)* particle formed in the Ni $(acac)_2$–$5AlEt_2(OEt)$ benzene hydrogenation at T = 120 °C and P_{H2} = 15 bar after 40 min of the reaction, *(b)* the particle-size distribution histogram and *(c)* the EDX spectrum. The inset in *(a)* is the selected area electron diffraction (SAED) pattern.

solution of nickel particles consisting of only a few atoms. Since the resolving power of the microscope used and the parameters of the carbonized copper gridsare were ~0.6–0.7 nm (see Experimental section), it was not possible to detect such particles at this stage of the study.

Thus, at this stage of research it can be assumed that the nanoscale particles of nickel or NiAl formed from $Ni(acac)_2$ and $AlEt_3$ with Al/Ni = 4 under catalytic hydrogenation conditions exhibited the highest activity in the benzene hydrogenation (TOF ≈ 3 min^{-1}, T = 120 °C, and P = 15 bar). The $Ni(acac)_2$–$AlEt_2(OEt)$ system was less active in the benzene hydrogenation (TOF = 0.86 min^{-1}, T = 120 °C, and P = 15 bar); however, its activity remained virtually constant for ratios in the range Al/Ni = 4–10, i.e., $AlEt_2(OEt)$ showed less inhibitory effect than $AlEt_3$. In addition, $AlEt_3$could undergo decomposition in the coordination sphere of nickel to form nickel aluminides in contrast with $AlEt_2(OEt)$. Note that at this stage of the study, it can not be ruled out that particles containing only a few nickel atoms can also have catalytic activity.

3.3. Results of the competitive hydrogenation method

The application of a method based on competitive reactions allows comparing the reactivity of arenes under strictly identical conditions. Therefore, for a better understanding of the arene hydrogenation kinetics using the $Ni(acac)_2$–$AlEt_3$ ($AlEt_2(OEt)$) systems, a study of the competitive hydrogenation reactions of benzene with toluene and/or three isomers of xylene was conducted.

In addition to the TOF values for the hydrogenation of benzene and a number of its alkyl substituted homologs, the results of the competitive hydrogenation of benzene with toluene and/or the three isomers of xylene at T = 120 °C and P_{H2} = 15 bar in the presence of the catalytic systems containing $AlEt_3$ or $AlEt_2(OEt)$ are presented in Table 2. It should be noted that the value of the hydrogenation reaction rate remains constant at very high levels of arene conversion. As a consequence, the constants of the adsorption equilibrium, i.e., the formation of the arene complex with the active catalytic centers, significantly exceed the values for the resulting naphthenes.

Table 2 shows that the values of the $[TOF_{benzene}]$:$[TOF_{alkylsubstitutedarene}]$ ratio are higher in the competitive hydrogenation experiments than those of the hydrogenation of individual arenes. These data indicate that the adsorption of benzene on the nickel surface (in its active hydrogenation forms) is preferred compared to the same value for alkyl-substituted arenes. The ratios between the K_{ads} (K_{ads} is the constant of adsorption) of benzene and the K_{ads} of alkyl arenes determined by the Smith method [52] (Supplementary Material (Appendix D.)) increase in the order toluene < *o*-xylene < *m*-xylene < *p*-xylene (Table 2, column 7).

These results are inconsistent with the arene hydrogenation mechanism originally proposed by Rooney and Völter [53,54], which included a π-complexation step between the arene and a transition metal. Thus, the increase in the degree of substitution of the benzene ring lowers the arene ionization potential, increasing the complexation constants of an arene with a transition metal.

The interpretation of catalytic reactions by means of transition metal-based schematic representations about the π-complex adsorption of arenes is advantageous over classical theories, as it permits to disclose the relationship between the real properties of aromatic reagents and catalysts [51,55]. It is believed, with varying degrees of validity, that benzenemay be present in at least three different forms that exist in equilibrium on the catalyst surface [56,57], namely, in the form of π- and σ-bonded surface complexes, as well as a π/σ-intermediate complex. The π- and π/σ-species are considered as reactive in the benzene hydrogenation, while the σ-species is thought to be inactive or a hydrogenation inhibiting form. Furthermore, it was postulated that the benzene molecule is preferably linked to one atom of nickel [58]. It should be noted that in the work of Agapie et al., direct experimental evidences for the potential direct coordination of nickel to the arenes were obtained [59–61].

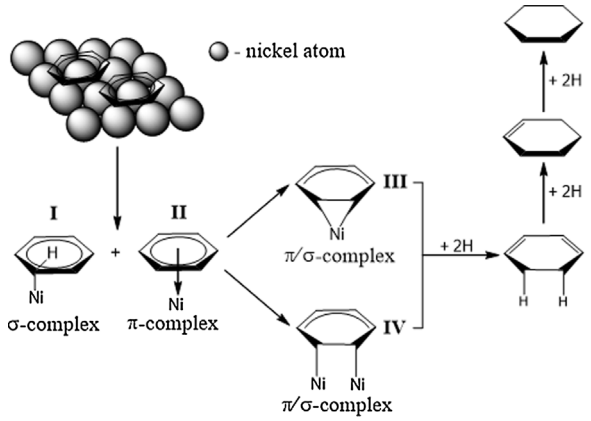

Scheme 1. Hydrogenation of arenes on nanoscale nickel catalysts at the example of benzene hydrogenation.

By combining the results obtained by the competitive experiments as well as the results published in [55–61] it was suggested that at the stage of the hydrogen attachment to the arene, the latter is not in the π-complex form II (Scheme 1), but in another form, such as the adsorbed π/σ-intermediate complex III and/or IV. This means that in the adsorbed state the destruction of the conjugated system II including the six π-electrons occurs. The step-by-step addition of six hydrogen atoms formed as a result of the dissociative adsorption of molecular hydrogen on the nickel atoms, is the rate-limiting step of the hydrogenation process.

The scheme presented by us is not a new mechanism; rather, it is more correct to consider the presented scheme as a compilation of several ideas proposed earlier [56–58], as well as the data already published [65–67] and the results obtained by us.

3.4. The stereochemistry of xylene hydrogenation

Finally, the stereochemistry of xylene hydrogenation, including under competitive hydrogenation conditions with benzene, was investigated.

It can be seen in Figs. 6 and 7 that the *cis/trans*-stereoisomeric ratio depends on the nature of the organoaluminium component of the catalyst for both individual xylene hydrogenation and mixtures of different xylenes with benzene under competitive hydrogenation conditions.

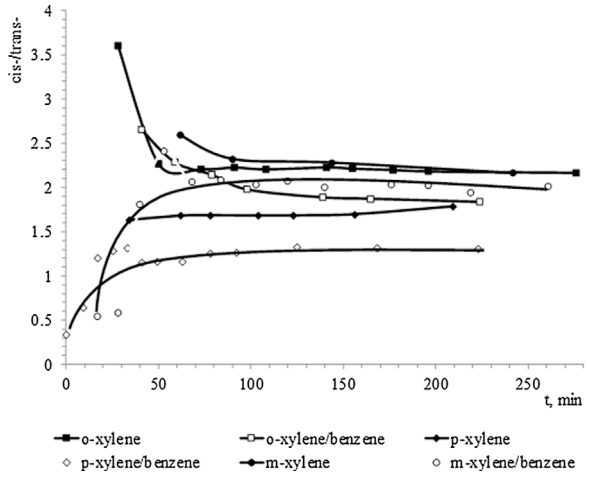

Fig. 6. The dependence of *cis/trans*-ratio on time of xylenes hydrogenation, including under competitive hydrogenation of xylene with benzene on $Ni(acac)_2$–$5AlEt_3$ catalytic system: [Ni] = $1{\cdot}10^{-2}$ mol/l, V = 40 ml, P_{H2} = 15 bar, T = 120 °C, ν_{xylene} = 0.292 mol (for hydrogenation of individual xylenes) and $\nu_{xylene.}/\nu_{benzene}$ = 1 (for competitive hydrogenation of benzene with xylenes).

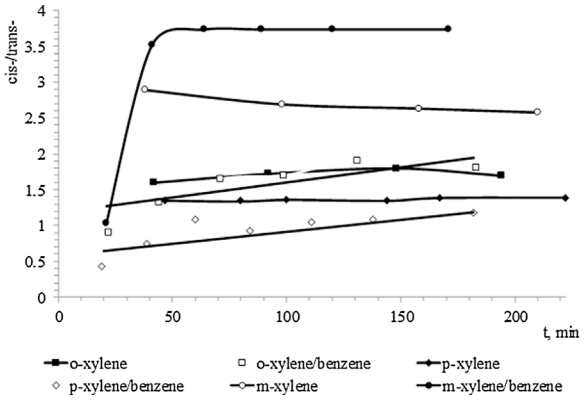

Fig. 7. The dependence of *cis/trans*-ratio upon time of xylenes hydrogenation, including under competitive hydrogenation of xylene with benzene on $Ni(acac)_2$–$5AlEt_2(OEt)$ catalytic system: [Ni] = $1{\cdot}10^{-2}$ mol/l, V = 40 ml, P_{H2} = 15 bar, T = 120 °C, ν_{xylene} = 0.292 mol (for hydrogenation of individual xylenes) and $\nu_{xylene.}/\nu_{benzene}$ = 1 (for competitive hydrogenation of benzene with xylenes).

Indeed, the *cis/trans*-ratio changes in the order *meta-* ≈ *ortho-* > *para*-xylene from 1.8–2.1 for 1,2- and 1,3-dimethylcyclohexane to 1.2–1.6 for 1,4-dimethylcyclohexane in the case of $AlEt_3$.

For the catalysts formed by the action of $AlEt_2(OEt)$, the ratio of *cis/trans*-dimethylcyclohexanes also decreased in the order 1,3- > 1,2- > 1,4-dimethylcyclohexane. In the initial stage, the *cis/trans*-ratio strongly depends on the hydrogenation time, and in hydrogenation of both individual *o*-xylene and its mixture with benzene, these values increase with time.

The time that is necessary for the *cis/trans*-ratio values to come to a steady-state segment is about 2 h, which substantially coincides with the output time to obtain constant values of TOF (Figs. 6 and 7). This result points to the decisive influence of the catalyst nature, most likely the size of the nanoparticles formed, with the coordination state of the surface nickel atoms being the main factor determining the hydrogenation stereoselectivity. The stereochemical distribution of the hydrogenation products clearly deviates from the thermodynamic equilibrium values and it is rather determined by kinetic factors. The *trans*-configuration is more stable in the case of 1,2- and 1,4-diastereomers, whereas for 1,3-derivatives an opposite trend can be found [42]. The stereochemistry of the xylene hydrogenation is determined by the ratio of the rate constants of hydrogen addition to intermediate hydrogenation product formation, as well as the rates of desorption and re-adsorption of these products [51]. The sequential addition of hydrogen atoms to the π/σ-adsorbed ring in the absence of an explicit rate-limiting step is described in the proposed schemes of the detailed mechanism of arene hydrogenation [62,63]. In different reports, the addition of the first [56,64], second [65], or sixth hydrogen atom is considered as the slow step. As described by Keane et el. [41,42], it is most likely that the addition of the first hydrogen atom to the adsorbed arene would be the rate-limiting step, because at this stage there is the greatest destabilization of the arene rings that is associated with the energy of the resonance.

The xylene molecules were adsorbed parallel to the surface and the two methyl groups were bent from surface in order to weak the steric repulsion.

The *cis/trans*-ratio was determined by the ratio of the rates of the successive addition of the hydrogen atoms to the adsorbed xylenes and the formation of the products of their partial hydrogenation. These rates in turn are dependent on the rates of hydrogen activation and the concentration of active hydrogen. A large array of experimental data reported in the literature indicates that an increase of hydrogen pressure leads to an increase of the *cis/trans* ratios of the diastereomers regardless of the nature of the catalyst. Therefore, during the first 2 h of hydrogenation the nanoparticle size and the state of the surface atom

layer change, when the hydrogen activation rate corresponds to the hydrogen addition rate.

o-Xylene was preferentially hydrogenated to *cis*-1,2-dimethylcyclohexane, although this ratio decreased markedly over time. Under such reaction conditions, *o*-xylene is most strongly held on the surface and the addition of the hydrogen atoms leads to the formation of the *cis*-product, as shown in the literature [42].

The hydrogenation of *m*-xylene led to the preferential formation of the *cis*-product, since it is the thermodynamically more stable stereoisomer compared to the 1,3-*trans*-product. This was confirmed by the fact that the value of the *cis/trans*-ratio reached high values both in the hydrogenation of the individual substrate and in its mixture with benzene in a competitive hydrogenation for all catalytic systems.

The steric hindrance is weaker in the case of *p*-xylene as compared with the previous two cases, resulting in values of *cis/trans*-ratio that are close to equimolar (Figs. 6 and 7). Therefore, it can be concluded that the *cis/trans*-ratio, as well as the TOF, is a fingerprint, i.e., a good indicator of the state of the catalyst surface layer, including the physical and chemical adsorption of the compounds of the catalytic systems, namely $AlEt_3$, $AlEt_2(acac)$, $AlEt_2(OEt)$, or AlEt(OEt)(acac). Thus, it seems appropriate to perform a further stoichiometry study of the hydrogenation of other arenes in the presence of nanosized nickel catalysts.

4. Conclusions

The hydrogenation TOFs of benzene and its methyl substituted homologs using two Ziegler catalyst systems based on $Ni(acac)_2$–$AlEt_3$ ($AlEt_2(OEt)$) at T = 80–120 °C, P_{H2} = 15 bar, and different Al/Ni ratios were determined in the present study for the first time. It was demonstrated that the TOF for the benzene hydrogenation was 0.03 min^{-1} at T = 120 °C and P_{H2} = 15 bar for the reduction of $Ni(acac)_2$ by hydrogen. It was found that the system based on $Ni(acac)_2$–$AlEt_3$ with Al/Ni = 4 was the most active in the arene hydrogenation (TOF_{C6H6} ≈ 3.0 min^{-1} at T = 120°C and P_{H2} = 15 bar). On the other hand, the TOF_{C6H6} for the $Ni(acac)_2$–$AlEt_2(OEt)$ system was 0.89 min^{-1}at T = 120 °C and P_{H2} = 15 bar in the wide range of ratios Al/Ni = 4–10. It was shown that the nanoscale particles of nickel and/or nickel aluminide exhibited catalytic activity in the hydrogenation of arenes in the case of the $Ni(acac)_2$–$AlEt_3$ systems, while for the $Ni(acac)_2$–$AlEt_2(OEt)$ systems only the nickel nanoparticles were active.

It is possible that the values of TOF described in the present work resulted from the presence of nickel particles consisting of only a few atoms in the solution. It was not possible to register such particles at this stage of the study. The previously stated hypotheses concerning the stereochemistry of the benzene hydrogenation on the nickel catalysts were confirmed by the results of kinetic experiments presented in the present article. Moreover, the mechanistic scheme for the arene hydrogenation that agrees with the experimental results was suggested.

Competitive hydrogenation reactions of benzene with toluene and three xylene isomers were also performed for the first time. The adsorption constants of toluene and the three isomers of xylene were determined relative to benzene and the stereochemistry of the hydrogen addition to the arene ring was illustrated. It was demonstrated that the *cis/trans*-stereoisomeric ratio depended on the nature of the organoaluminium component of the catalyst for both individual xylene hydrogenation and mixtures of different xylenes with benzene under competitive hydrogenation conditions. The available kinetic data allowed us to suggest that the *cis/trans*–stereoisomeric ratio is a good indicator of the state of the catalyst surface layer, including the physical and chemical adsorption of the compounds of the catalytic systems, namely organoaluminium components of considered catalytic systems. Therefore, at the next stage of the research, in addition to demonstration of the true nature of the catalytic activity, it is planned to study the stoichiometry of the hydrogenation of other arenes in the presence of Ni $(acac)_2$-$AlEt_3$ ($AlEt_2(OEt)$) catalytic systems.

References

[1] G. Vilé, D. Albani, N. Almora-Barrios, N. López, J. Pérez-Ramírez, ChemCatChem 8 (2015) 21–33.
[2] W.M. Alley, C.W. Girard, S. zkar, R.G. Finke, Inorg. Chem. 48 (2009) 1114–1121.
[3] W.M. Alley, I.K. Hamdemir, Q. Wang, A.I. Frenkel, L. Li, J.C. Yang, L.D. Menard, R.G. Nuzzo, S. zkar, K.A. Johnson, R.G. Finke, Inorg. Chem. 49 (2010) 8131–8147.
[4] W.M. Alley, I.K. Hamdemir, Q. Wang, A.I. Frenkel, L. Li, J.C. Yang, L.D. Menard, R.G. Nuzzo, S. Ozkar, K.-H. Yih, K.A. Johnson, R.G. Finke, S. Zkar, Langmuir 27 (2011) 6279–6294.
[5] I.K. Hamdemir, S. Özkar, R.G. Finke, J. Mol. Catal. A Chem. 378 (2013) 333–343.
[6] F.K. Shmidt, L.O. Nindakova, B.A. Shainyanb, V.V. Saraev, N.N. Chipaninab, V.A. Umanetz, J. Mol. Catal. A. Chem. 235 (2005) 161–172.
[7] L.O. Nindakova, F.K. Shmidt, V.V. Saraev, B.A. Shainyan, N.N. Chipanina, V.A. Umanets, L.N. Belonogova, D.S.D. Toryashinova, Kinet. Catal. 47 (2006) 54–63.
[8] H. Bönnemann, R.M. Richards, M.R. Ryan, H. Bönnemann, Eur. J. Inorg. Chem. 2001 (2001) 2455–2480.
[9] K. Angermund, M. Bohl, E. Dinjus, U. Endruschat, F. Gassner, H.G. Haubold, J. Hormes, G. Kohl, F.T. Mauschick, H. Modrow, R. Mortel, R. Mynott, B. Tesche, T. Vad, N. Waldofner, H. Bonnemann, Angew. Chem. Int. Ed. 41 (2002) 4041–4044.
[10] L.B. Belykh, Y.Y. Titova, V.A. Umanets, A.V. Rokhin, F.K. Schmidt, Appl. Catal. A Gen. 401 (2011) 65–72.
[11] F.K. Schmidt, Y.Y. Titova, S.S. Kolesnikov, L.B. Belykh, Appl. Catal. A. Gen. 499 (2015) 177–187.
[12] J.G. de Vries, C.J. Elsevier (Eds.), The Handbook of Homogeneous Hydrogenation, Wiley-VCH, Weinheim, 2008.
[13] F.K. Shmidt, Kataliz Kompleksami Metallov Pervogo Perekhodnogo Ryada Reaktsii Gidrirovaniya I Dimerizatsii (Hydrogenation and Dimerization Catalyzed by Complexes of First Row Transition Metals), Irkutsk. Gos. Univ., Irkutsk, 1986.
[14] J.A. Widegren, R.G. Finke, J. Mol. Catal. A. Chem. 191 (2003) 187–207.
[15] Y.Y. Titova, L.B. Belykh, F.K. Shmidt, Kinet. Catal. 57 (2016) 388–393.
[16] Y.Y. Titova, L.B. Belykh, F.K. Shmidt, Kinet. Catal. 57 (2016) 344–353.
[17] S.J. Lapporte, W.R. Schuett, J. Org. Chem. 28 (1963) 1947–1948.
[18] K.R. Januszkiewicz, H. Alper, Organometallics 2 (1983) 1055–1057.
[19] B. Schuldt, D. Heller, F. Storz, J. Mol. Catal. 81 (1993) 195–206.
[20] F. Storz, D. Heller, K. Madeja, J. Mol. Catal. 84 (1993) 33–38.
[21] J. Schulz, a Roucoux, H. Patin, Chemistry 6 (2000) 618–624.
[22] J.A. Widegren, R.G. Finke, Inorg. Chem. 41 (2002) 1558–1572.
[23] J.A. Widegren, R.G. Finke, J. Mol. Catal. A. Chem. 191 (2003) 187–207.
[24] P.J. Dyson, Dalt Trans. 15 (2003) 2964–2974.
[25] N.T. McManusa, G.L. Rempel, J. Macromol. Sci. Part C Polym. Rev. 35 (1995) 239–285.
[26] M. Baerns, Basic Principles in Applied Catalysis, Springer- Verlag, Berlin, 2004.
[27] R. Velichkova, V. Toncheva, C. Antonov, V. Alexandrov, S. Pavlova, L. Dubrovina, E. Gladkova, J. Appl. Polym. Sci. 42 (1991) 3083–3090.
[28] H. Li, Y. Xu, Mater. Lett. 51 (2001) 101–107.
[29] V. Aruna, N. Sridevi, P.P. Robinsona, S. Manjua, K.K.M. Yusuff, N.S.V. Aruna, P.P. Robinsona, S. Manjua, K.K.M. Yusuff, J. Mol. Catal. A. Chem. 304 (2009) 191–198.
[30] L. Zhu, H. Sun, H. Fu, J. Zheng, N. Zhang, Y. Li, B.H. Chen, Appl. Catal. A Gen. 499 (2015) 124–132.
[31] A.J. Gordon, R.A. Ford, Handbook of Practical Data, Techniques, and References, Wiley, New York, 1972.
[32] J. Mitchell, D.M. Smith, Aquametry, Wiley, New York, 1977.
[33] W. Polaczkowa (Ed.), Preparatykaorganiczna, Pracazbiorowa, Warsaw, 1954.
[34] D.D. Perrin, W.L.F. Armaregov, Purification of Laboratory Chemicals, 3rd ed., Pergamon Press, Oxford, 1988.
[35] F.K. Schmidt, Y.Y. Titova, L.B. Belykh, Kinet. Catal. 56 (2015) 582–591.
[36] D.Y. Murzin, S. Smeds, Tapio Salmi, React. Kinet. Catal. Lett. 71 (2000) 47–54.
[37] D.Y. Murzin, T. Salmi, Catalytic Kinetics, Elsevier Science, 2005.
[38] S. Siegel, G.V. Smith, B. Dmuchovsky, D. Dubbell, W. Halpern, J. Am. Chem. Soc. 84 (1962) 3136–3139.
[39] M. Vasiur Rahaman, M. Albert Vannice, J. Catal. 127 (1991) 267–275.
[40] J. Völter, M. Hermann, K. Heise, J. Catal. 12 (1968) 307–313.
[41] M.A. Keane, P.M. Patterson, J. Chem. Soc. Faraday Trans. 92 (1996) 1413–1421.
[42] M.A. Keane, J. Catal. 166 (1997) 347–355.
[43] F.K. Shmidt, Y.Y. Titova, L.B. Belykh, Kinet. Catal. 56 (2015) 574–583.
[44] F.K. Schmidt, T.V. Dmitrieva, G.V. Ratovskii, Koord. Khim. 10 (1984) 213–221.
[45] J.G. van Ommen, J.G.M. van Rens, P.J. Gellings, J. Mol. Catal. 13 (1981) 313–321.
[46] D. Bogg, M. Conyngham, J.M. Corker, A.J. Dent, J. Evans, R.C. Farrow, V.L. Kambhampati, A.F. Masters, D.N. McLeod, C.A. Ramsdale, N. Mcleod, C.A. Ramsdale, Chem. Commun. 5 (1996) 647–648.
[47] H. Bönnemann, N. Waldöfner, H.-G. Haubold, T. Vad, Chem. Mater. 14 (2002) 1115–1120.
[48] W.M. Alley, I.K. Hamdemir, K. a. Johnson, R.G. Finke, W.M. Alleya, I.K. Hamdemira, K.A. Johnsonb, R.G. Finke, J. Mol. Catal. A. Chem. 315 (2010) 1–27.
[49] A.B. Crooks, K.-H. Yih, L. Li, J.C. Yang, S. Özkar, R.G. Finke, ACS Catal. 5 (2015) 3342–3353.
[50] M. Aliofkhazraei (Ed.), Handbook of Nanoparticles, Springer International Publishing, Switzerland, 2015.
[51] K.S. Weddle, J.D. Aiken III, R.G. Finke, J. Am. Chem. Soc. 120 (1998) 5653–5666.
[52] C.P. Rader, H.A. Smith, J. Am. Chem. Soc. 84 (1962) 1443–1449.
[53] J. Rooney, J. Catal. 2 (1963) 53–57.

[54] J. Völter, J. Catal. 3 (1964) 297–298.
[55] J. Mortier, Arene Chemistry: Reaction Mechanisms and Methods for Aromatic Compounds, John Wiley & Sons, Inc., 2016.
[56] R.B. Moyes, P.B. Wells, Adv. Catal. 23 (1973) 121–156.
[57] K.H.V. Prasad, K.B.S. Prasad, M.M. Mallikarjunan, R. Vaidyeswaran, J. Catal. 84 (1983) 65–73.
[58] H. Jobic, J. Tomkinson, J.P. Candy, P. Fouilloux, A.J. Renouprez, Surf. Sci. 95 (1980) 496–510.
[59] A. Velian, S. Lin, A.J.M. Miller, M.W. Day, T. Agapie, J. Am. Chem. Soc. 132 (2010) 6296–6297.
[60] S. Lin, M.W. Day, W. Michael, T. Agapie, J. Am. Chem. Soc. 133 (2011) 3828–3831.
[61] S. Suseno, K.T. Horak, M.W. Day, T. Agapie, Organometallics 32 (2013) 6883–6886.
[62] Yu. Snagovskii, G.D. Lyubarskii, G.M. Ostrovskii, Kinet. Katal 7 (1966) 232–240.
[63] R.Z.C. van Meerten, J.W.E. Coenen, J. Catal. 46 (1977) 13–24.
[64] S. Zrncevic, D. Rusic, Chem. Sci. Eng. 43 (1988) 763–767.
[65] M.V. Rahaman, M.A. Vannice, J. Catal. 127 (1991) 275–267.